miR-17~92 family microRNAs are critical regulators of T follicular helper cell differentiation

Seung Goo Kang, Wen-Hsien Liu, Peiwen Lu, Hyun Yong Jin, Hyung W. Lim, Jovan Shepherd, Daniel Fremgen, Eric Verdin, Michael B. A. Oldstone, Hai Qi, John R. Teijaro, Changchun Xiao

Supplementary Figures 1-9

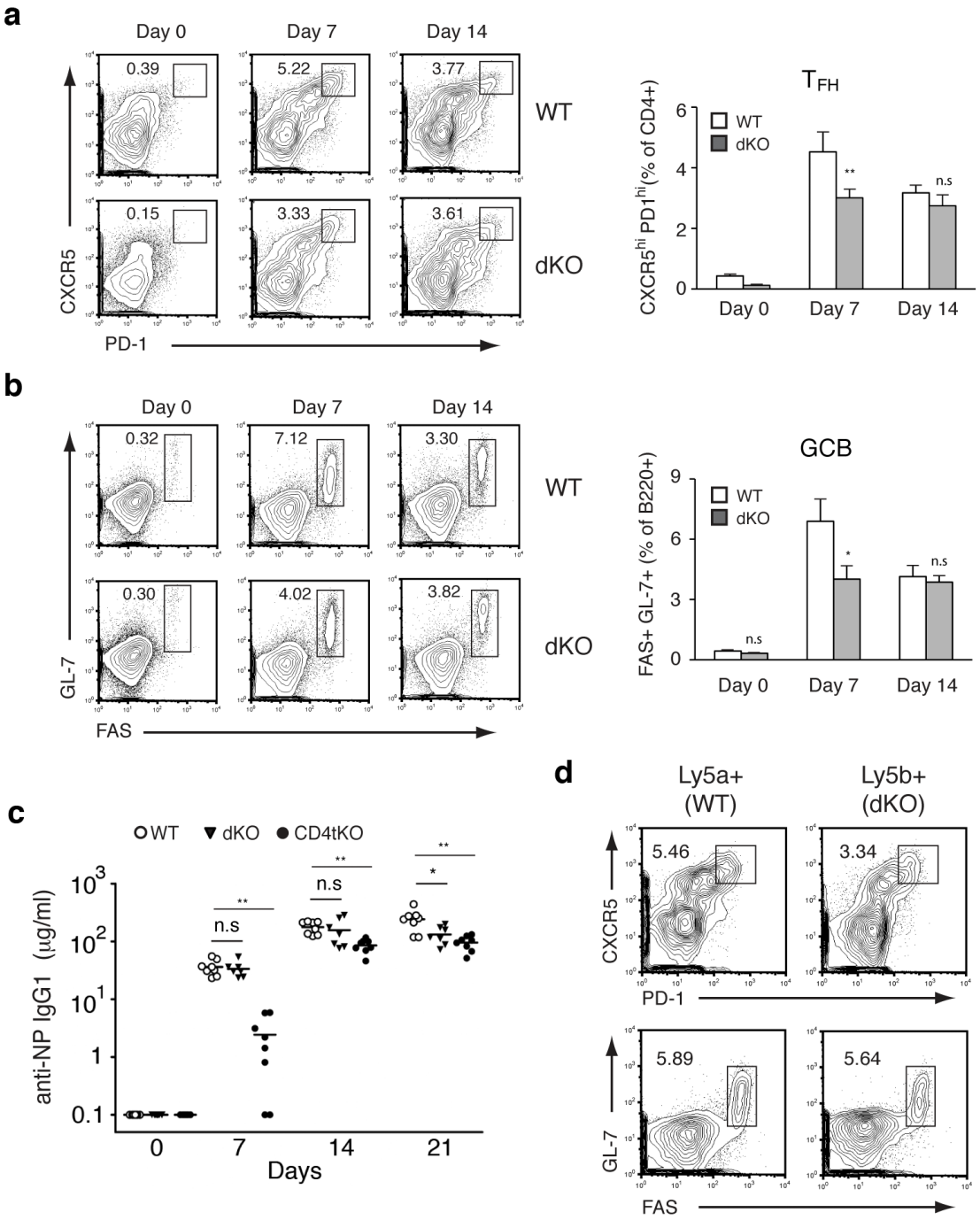

Supplementary Figure 1. T_{FH} differentiation, GCB formation, and antibody production in dKO mice. (**a,b**) Flow cytometry analysis of T_{FH} (**a**) and GCB (**b**) cell differentiation in WT and dKO mice at days 7 and 14 after immunization with NP-OVA+Alum+LPS (n=6 per group). (**c**) NP-specific IgG1 antibody production was determined by ELISA at indicated times after NP-CGG+Alum immunization (i.p). WT and CD4tKO results are also depicted in Fig. 1f. (**d**) Mixed bone marrow chimeras (Ly5a WT:Ly5b dKO=1:1) were immunized with NP-OVA+Alum+LPS (i.p). T_{FH} (upper) and GCB (lower) cell differentiation was analyzed at day 7 after immunization. All graphs are shown as means ± s.e.m. *, $p < 0.05$; **, $p < 0.01$.

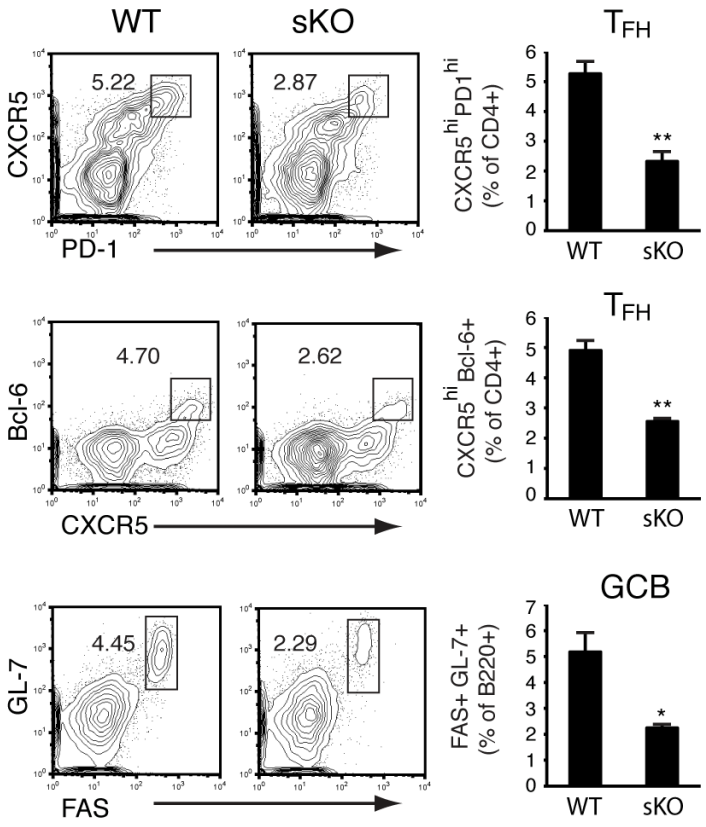

Supplementary Figure 2. T_{FH} and GCB differentiation in miR-17~92 single KO mice. Flow cytometry analysis of $CXCR5^{+}PD1^{+}$ T_{FH} (upper), $CXCR5^{+}Bcl\text{-}6^{+}$ T_{FH} (middle), and $FAS^{+}GL\text{-}7^{+}$ GCB (lower) cell development in WT and sKO mice ($CD4Cre;miR\text{-}17\sim92^{fl/fl}$) at day 7 after immunization with NP-OVA+Alum+LPS (i.p.) (n=3 per group). All graphs are shown as means ± s.e.m. *, $p < 0.05$; **, $p < 0.01$.

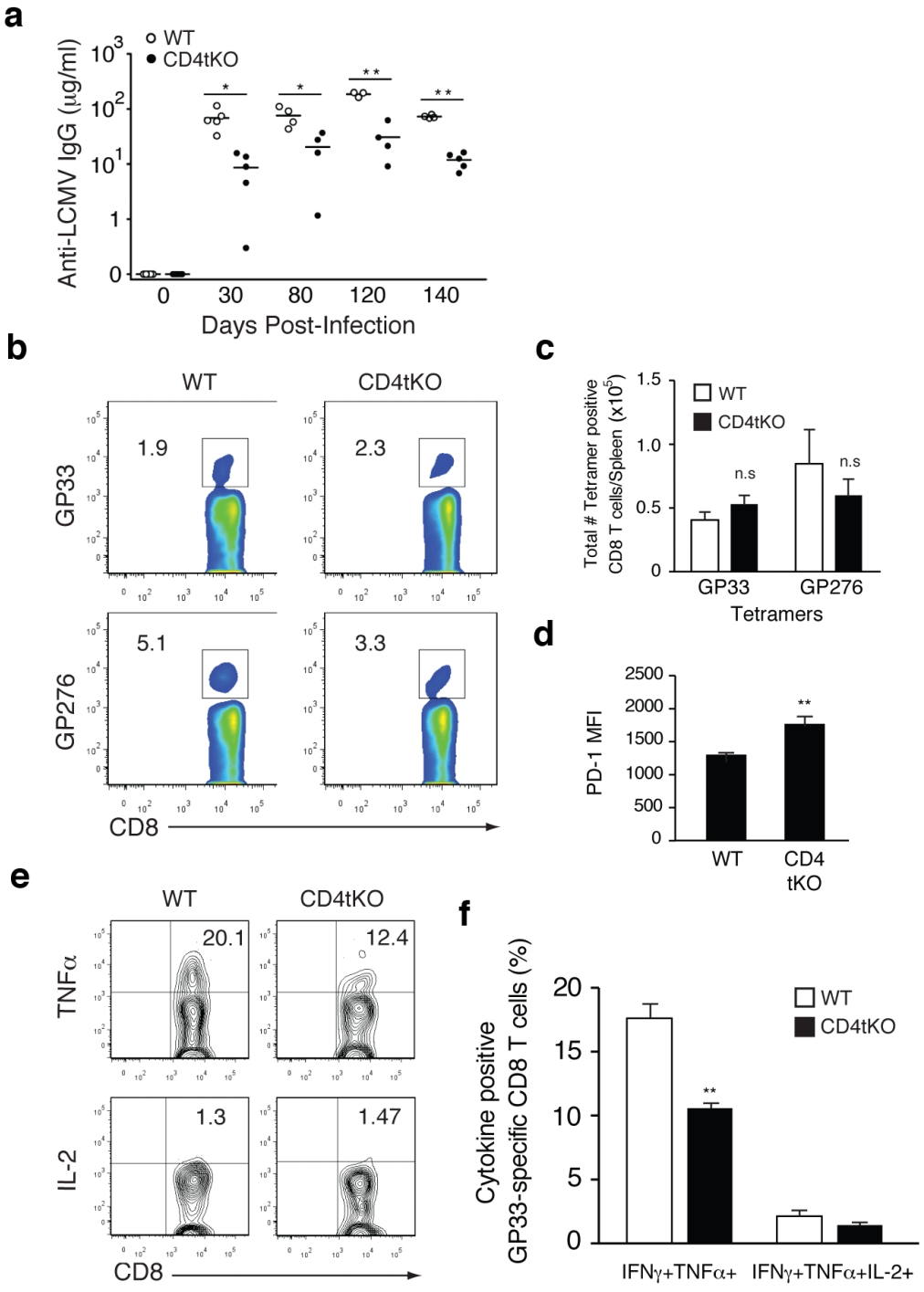

Supplementary Figure 3. Immune responses in CD4tKO mice during chronic virus infection. (**a**) Anti-LCMV IgG antibody concentration was determined by ELISA at indicated time points after LCMV C13 infection. (**b,c**) Frequency (**b**) and total numbers (**c**) of GP^{33-44}- and $GP^{276-286}$-specific $CD8^+$ T cells at day 30 following LCMV clone-13 infection. (**d**) Mean fluorescent intensity (MFI) of PD-1 expression on GP^{33-44}-specific $CD8^+$ T cells at day 30 post-infection. (**e**) Flow cytometry analysis of GP^{33-44}-specific $CD8^+$ T cell cytokine production. Graphs are gated on IFN-γ+ GP^{33-44}-specific $CD8^+$ T cells. (**f**) Percentages of cytokine producing GP^{33-44}-specific $CD8^+$ T cells at day 30 post infection. All graphs are shown as means ± s.e.m. *, $p < 0.05$; **, $p < 0.01$.

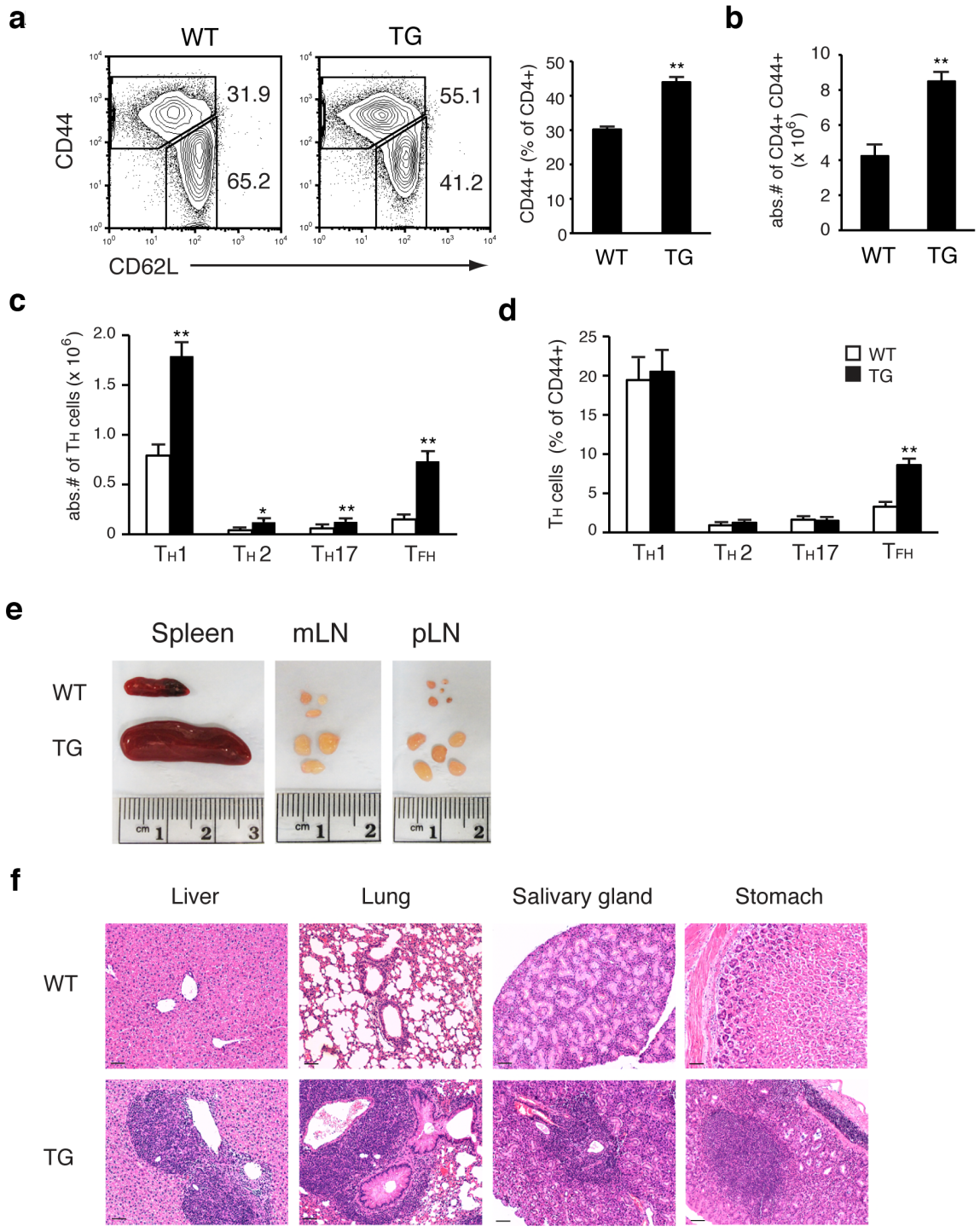

Supplementary Figure 4. T cell-specific miR-17~92 transgenic mice developed fatal immunopathology. (**a-d**) The activation status of $CD4^+$ T cells (**a**), $CD4^+CD44^+$ T cell numbers (**b**), total numbers (**c**) and frequency (**d**, plotted as percentages of $CD4^+CD44^+$ T cells) of T_H1, T_H2, T_H17, and T_{FH} cells in the spleen of 6-8 week old non-immunized mice. (**e**) Splenomegaly and lymphadenopathy in 6-8 month old TG mice. mLN, mesenteric lymph nodes. pLN, peripheral lymph nodes. (**f**) Hematoxylin and eosin staining of liver, lung, salivary gland, and stomach of 6-8 month old mice. Note mononuclear cell infiltration in non-lymphoid tissues in TG mice. Scale bar, 100 μm. All graphs are shown as means ± s.e.m. *, $p < 0.05$; **, $p < 0.01$.

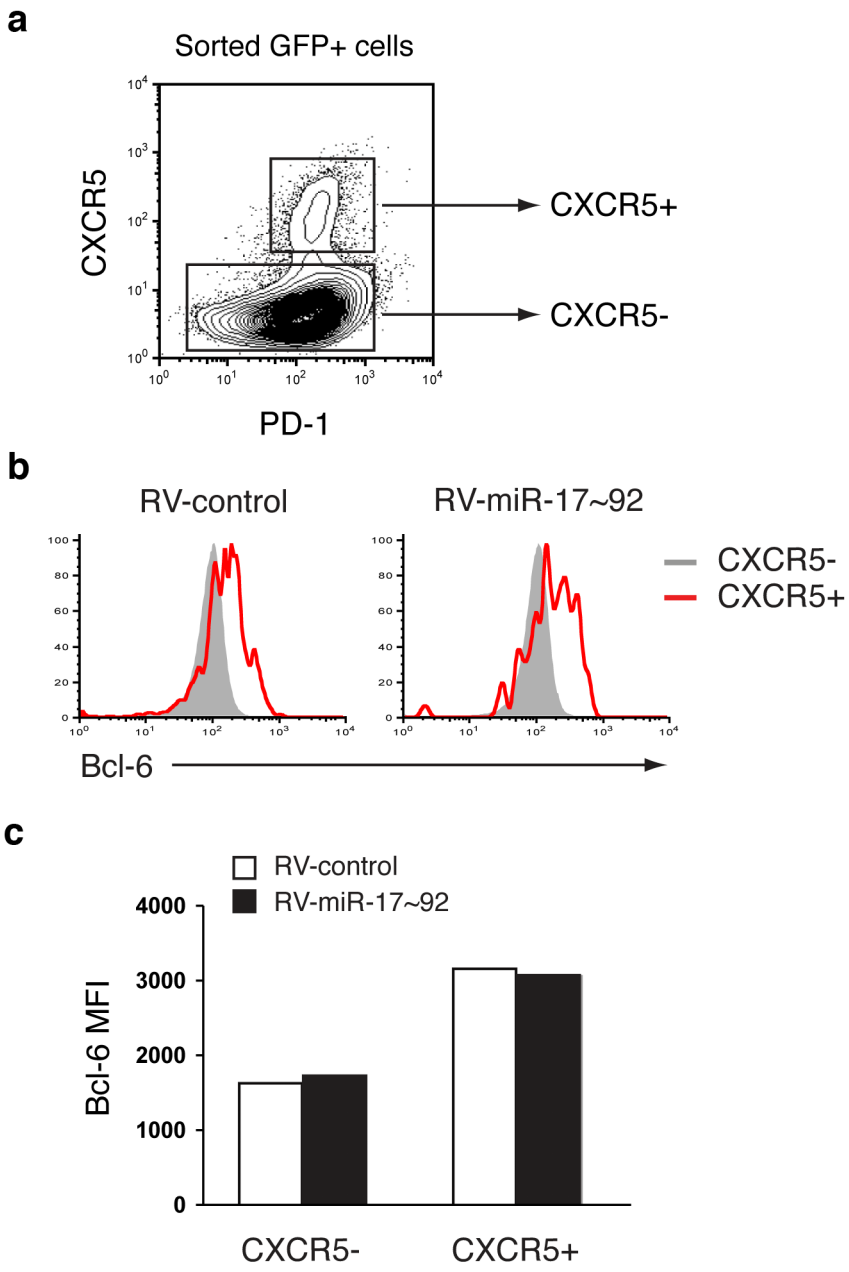

Supplementary Figure 5. Bcl-6 expression in miR-17~92 over-expressing CD4$^+$ T cells. WT naïve CD4$^+$ T cells were transduced with RV-control or RV-miR-17~92 and activated *in vitro* for T_{FH} differentiation. GFP$^+$ cells were sorted and stained for CXCR5, PD1 and Bcl-6. Expression level of Bcl-6 in CXCR5$^+$PD1$^+$ T_{FH} or CXCR5$^-$PD1$^{+/-}$ T cells (**a**) was examined by flow cytometry analysis and presented as histogram (**b**) and mean fluorescent intensity (**c**) (representatives of two independent experiments).

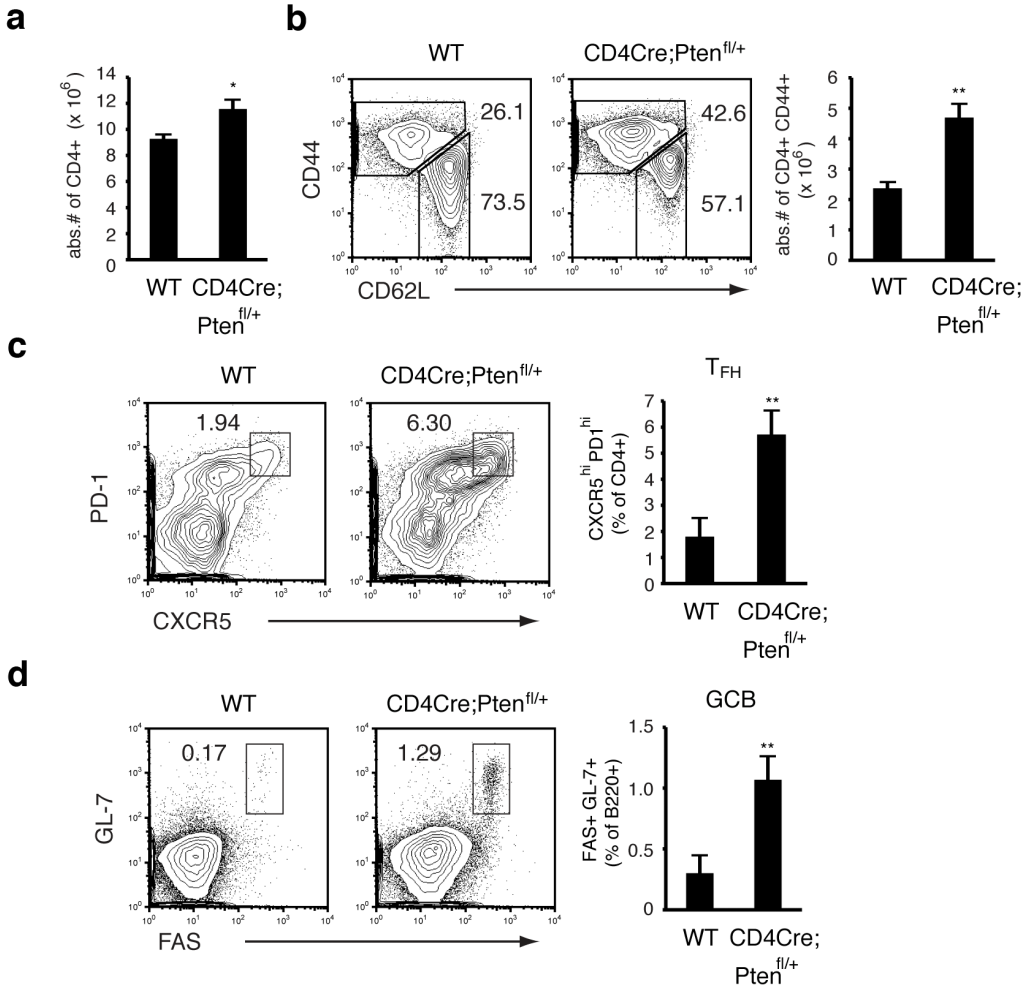

Supplementary Figure 6. T cell-specific deletion of one copy of the Pten gene causes spontaneous germinal center reaction. (**a-d**) Flow cytometry analysis of 8~9 month old non-immunized WT and CD4Cre;Pten$^{f/+}$ mice (n=8 for WT, n=13 for CD4Cre;Pten$^{f/+}$). Total numbers of CD4$^+$ (**a**) and CD4$^+$CD44$^+$ (**b**) T cells in the spleen are summarized in bar graphs. Flow cytometry analysis of CD4$^+$CD44$^+$ (**b**), CXCR5^{hi} PD-1^{hi} T_{FH} (**c**) and FAS$^+$GL-7$^+$ GCB cells (**d**) in the spleen. (**b-c**), gated on CD4$^+$ T cells. (**d**), gated on B220$^+$ B cells. All graphs are shown as means ± s.e.m. *, $p < 0.05$; **, $p < 0.01$.

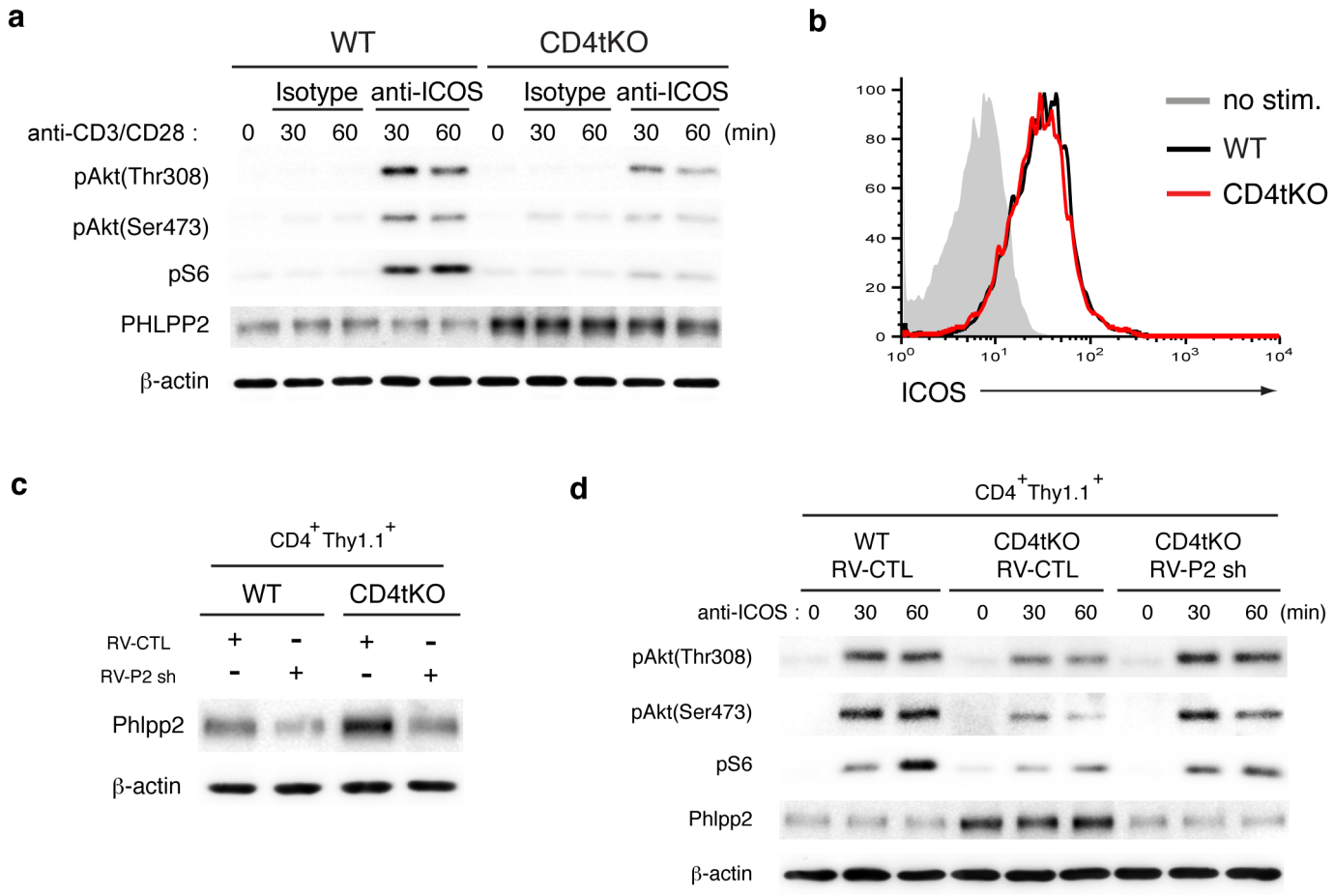

Supplementary Figure 7. Phlpp2 knockdown restores ICOS-mediated PI3K signaling in CD4tKO CD4$^+$ T cells. (**a**) WT and CD4tKO naïve CD4$^+$ T cells were activated *in vitro* with anti-CD3/CD28 for 3 days and rested in serum free media for 3 hours. Cells were treated with agonist hamster anti-ICOS or isotype antibody followed by anti-hamster IgG antibody treatment for indicated amounts of time. pAkt, pS6 and Phlpp2 levels were examined by Western blot. (**b**) CD4$^+$ T cells from (**a**) were examined for ICOS expression level on cell surface by flow cytometry. (**c,d**) *in vitro* activated WT and CD4tKO CD4$^+$ T cells were transduced with Thy1.1-expressing RV-CTL or RV-Phlpp2 shRNA (RV-P2 sh) retrovirus and Thy1.1$^+$ cells were isolated at day 3 after activation and infection and examined for Phlpp2 protein level by Western blot (**c**). Isolated Thy1.1+ cells were rested for 3 hours in the absence of activation, re-stimulated with anti-ICOS, and analyzed as described in (**a**). Data are representatives of two (**b**) and three (**a**, **c** and **d**) independent experiments.

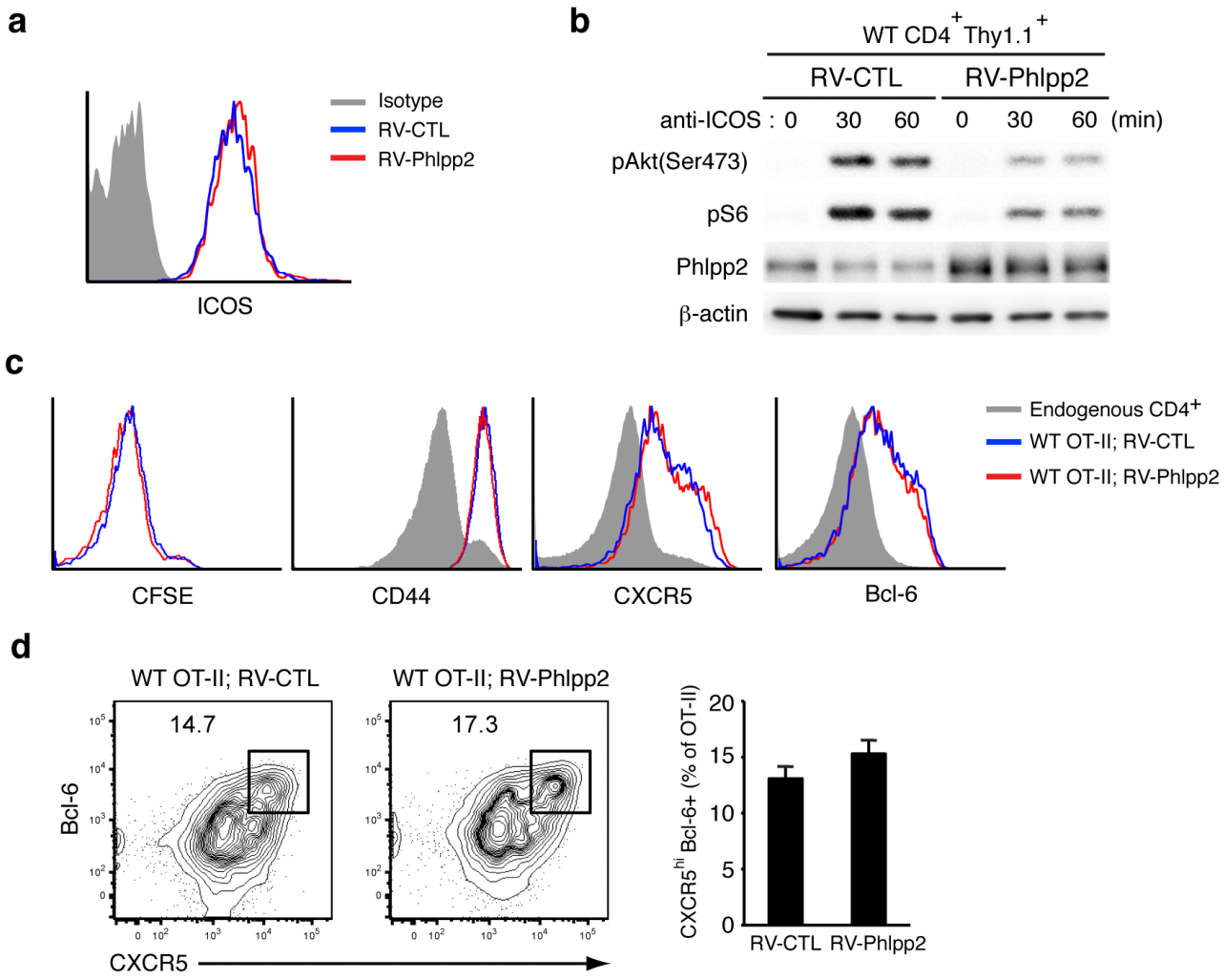

Supplementary Figure 8. Phlpp2 overexpression impairs ICOS-PI3K signaling, but does not affect CD4$^+$ T cell proliferation, activation, or CXCR5 and Bcl-6 expression. (**a-b**) *in vitro* activated WT naive CD4$^+$ T cells were transduced with Thy1.1-expressing RV-CTL or RV-Phlpp2 retrovirus. Thy1.1$^+$ cells were purified on day 3 after activation and infection, rested for 3 hours in serum free media. ICOS expression on cell surface was examined by flow cytometry (**a**). Rested cells were stimulated with anti-ICOS for indicated amounts of time, and pAkt and pS6 were examined by Western blot (**b**). (**c-d**) Thy1.1$^+$ cells were purified from RV-CTL or RV-Phlpp2 retrovirus infected WT OT-II CD4$^+$ T cells, labeled with CFSE, adoptively transferred into B6.Ly5a mice, followed by s.c. OVA+Alum immunization. OT-II CD4$^+$ T cell proliferation and expression of surface markers and Bcl-6 were examined on day 4 after immunization in draining lymph nodes. Graph is shown as means ± s.e.m.

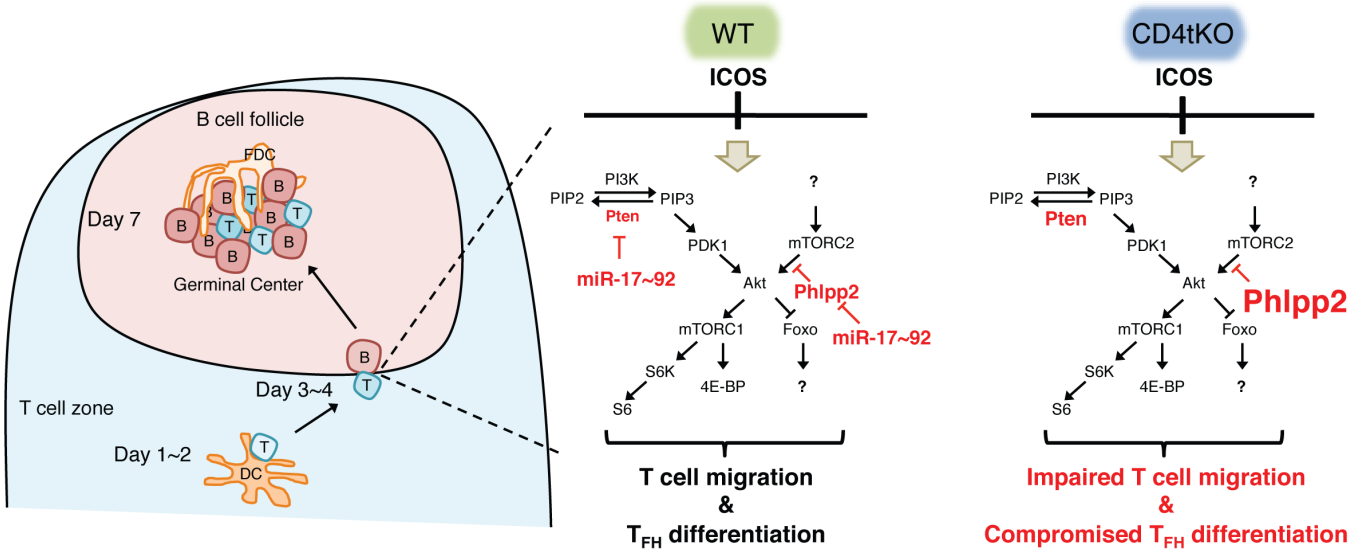

Supplementary Figure 9. Schematic depiction of miR-17~92 family miRNA-mediated regulation of T_{FH} differentiation. The expression levels of both miR-17~92 family miRNAs and their target gene Phlpp2 are low in naive $CD4^+$ T cells. They are significantly induced upon T cell activation, peak around day 2, and are downregulated afterwards. The upregulation of miR-17~92 family miRNA expression serves to limit the activation-induced Phlpp2 protein to a proper range. In CD4tKO $CD4^+$ T cells, the Phlpp2 protein level remains high on day 3, resulting in compromised ICOS-PI3K signaling, and inability of T cells to migrate into B cell follicles and to differentiate into T_{FH} cells. Note that the font sizes of Pten, Phlpp2, and miR-17~92 indicate their relative expression levels during T_{FH} differentiation.